

LA-UR- 11-00617

Approved for public release;
distribution is unlimited.

Title: Future Perspectives of Using Hollow Fibers as Structured Packings in Light Hydrocarbon Distillation

Author(s): Dali Yang, Ronald Martinez, Bruce Orler, Stephanie Tornga, Cindy Welch, and Loan Le

Intended for: 2011 AIChE Spring Meeting 2011, Chicago, U.S.A.
March 13-18, 2011



Los Alamos National Laboratory, an affirmative action/equal opportunity employer, is operated by the Los Alamos National Security, LLC for the National Nuclear Security Administration of the U.S. Department of Energy under contract DE-AC52-06NA25396. By acceptance of this article, the publisher recognizes that the U.S. Government retains a nonexclusive, royalty-free license to publish or reproduce the published form of this contribution, or to allow others to do so, for U.S. Government purposes. Los Alamos National Laboratory requests that the publisher identify this article as work performed under the auspices of the U.S. Department of Energy. Los Alamos National Laboratory strongly supports academic freedom and a researcher's right to publish; as an institution, however, the Laboratory does not endorse the viewpoint of a publication or guarantee its technical correctness.

Future Perspectives of Using Hollow Fibers as Structured Packings in Light Hydrocarbon Distillation

Dali Yang (dyang@lanl.gov, 505-665-4054), Bruce Orler, Cindy Welch, Stephanie Tornga, Loan Le, and Ronald Martinez
Los Alamos National Laboratory, Los Alamos, NM 87545, U.S.A

Introduction

Olefin and paraffin are the largest chemical commodities. Furthermore, they are major building blocks for the petrochemical industry. Each year, petroleum refining, consumes 4,500 TBtu/yr in separation energy, making it one of the most energy-intensive industries in the United States¹. Just considering liquefied petroleum gas (ethane/propane/butane) and olefins (ethylene and propylene) alone, the distillation energy consumption is about 400 TBtu/yr in the US. Since petroleum distillation is a mature technology, incremental improvements in column/tray design will only provide a few percent improvements in the performance. However, each percent saving in net energy use amounts to savings of 10 TBtu/yr and reduces CO₂ emissions by 0.2 MTon/yr^{2,3}. In practice, distillation columns require 100 to 200 trays to achieve the desired separation. The height of a transfer unit (HTU) of conventional packings is typical in the range of 36 – 60 inch⁴. Since 2006, we had explored using several non-selective membranes as the structured packings to replace the conventional packing materials used in propane and propylene distillation. We obtained the lowest HTU of < 8 inch for the hollow fiber column⁵⁻⁷, which was >5 times shorter than that of the conventional packing materials. In 2008, we also investigated this type of packing materials in iso-/n-butane distillation⁸. Because of a slightly larger relative volatility of iso-/n-butane than that of propane/propylene, a wider and a more stable operational range was obtained for the iso-/n-butane pair. However, all of the experiments were conducted on a small scale with flowrate of < 25 gram/min. Recently, we demonstrated this technology on a larger scale (<250 gram/min). Within the loading range of F-factor < 2.2 Pa^{0.5}, a pressure drop on the vapor side is below 50 mbar/m, which suggests that the pressure drop of hollow fibers packings is not an engineering barrier for the applications in distillations. The thermal stability study suggests that polypropylene hollow fibers are stable after a long time exposure to C₂ – C₄ mixtures. The effects of packing density on the separation efficiency will be discussed.

Experimental

In this work, we have constructed an new distillation apparatus, which can be operated at the flowrate up to 250 gram/min. Compared to our old system^{5,8}, it was scaled for up to 10 times. The apparatus was comprised of reboiler, hollow fiber column, condenser, heat exchanger, circulation pump, auto-sampling system, catch tank, four mass flowmeters, two pressure differential pressure gauges, five pressure gauges, and many thermal couples. The operational parameters were recorded by Labview program in real time. The auto-sampling system was controlled by Labview program as well. A certain amount of iso-/n-butane mixture was fed into the reboiler. By controlling the temperature difference between reboiler and condenser, the process flowrate and temperature were controlled. When we divided some portion of liquid into the catch tank, we could mimic the operations under the changeable reflux ratio condition in addition to the total reflux ratio condition. A circulation pump was added between the condenser and the membrane column, which ensured the liquid flow direction. The mixture of iso-/n-butane (50%/50%) was purchased from Trigas (Irving, TX). Ultra-pure helium and argon (>99.99%) were used as Micro-GC mobile phases. Two standards (propylene/propane and iso-/n-butane mixtures) were used to calibrate the micro-GC (Agilent).

Hollow modules were made of Celgard® polypropylene (PP) hollow fiber with 240 μm ID and 30 μm wall. The fiber porosity was $\sim 40\%$. To investigate the effect of the packing density on the module performance, the packing density varied from 5.5 to 18.5%. The module length was about one meter.

To evaluate the thermal stability of the polypropylene hollow fibers, the fibers were immersed in iso-/n-butane mixture, benzene, and cyclohexane at 50 °C for different times. The thermal gravimetric analysis (TGA), differential scanning calorimetry (DSC), dynamic mechanical analysis (DMA), and other related characterizations of the aged samples were conducted to determine the effect of solvent exposure on the thermal, the mechanical and the morphological properties of the hollow fibers.

Results and Discussion

1. Capacity of hollow fiber modules

In the olefin/paraffin systems, (e.g. ethane/ethylene, propane/propylene, and n-butane/iso-butane), flooding is commonly encountered when the column is operated at a high capacity. This is because the columns are operated under conditions where the gas and liquid densities are similar. Therefore, the flooding is a more severe restriction. Therefore, lack of flooding is especially important for the new type of structured packing materials when they can be used at the high capacity condition. Generally, the capacity of the packing materials can be determined by the correlation between flow parameter and capacity factor. The flow parameter can be calculated using:

$$\text{Flow parameter} = \left(\frac{L'}{G'} \right) \left(\frac{\rho'_G}{\rho'_L} \right)^{0.5}, \quad (1)$$

where L' and G' are the liquid and gas mass fluxes (lb/s ft^2), respectively, and ρ'_L and ρ'_G are the liquid and vapor density (lb/ft^3), respectively. The capacity factor depends on the ratio of the kinetic energy in the vapor to the potential energy in the liquid, which is defined as:

$$\text{Capacity factor} = \frac{G'^2 F \psi \eta^{0.2}}{\rho'_G \rho'_L g_c} \quad (2)$$

where F is the packing factor (ft^{-1}), ψ is the density ratio between water and process liquid, η is the viscosity (cP) of process liquid, g_c is the gravitational constant ($32.2 \text{ lb-ft/lb_f-sec}^2$).

Capacity factors and flow parameters for the five hollow fiber modules are plotted in Figure 1, where the solid line gives the up-limit capacity of conventional packing materials. However, in the hollow fiber packing both liquid and vapor have their own channels in which to flow, so the flooding encountered in a conventional packed tower is circumvented. Thus most of our experimental points lie above this solid flooding line. This means that hollow fiber modules can be over at least 10 times more productive per unit volume than conventional packing.

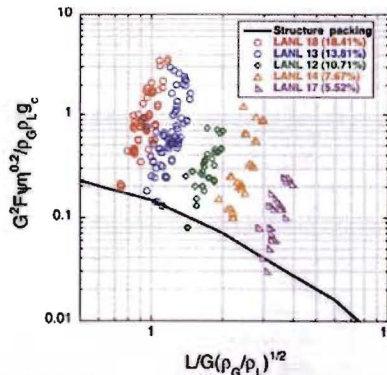


Figure 1. The correlation of flow parameter vs. capacity factor for five hollow fiber modules (the operation conditions range from 15 – 40 °C, and 30 – 80 psig for n-/iso-butane system).

In general, the flow parameter is related to the cross-sectional area ratio of vapor to liquid phase. Lower packing density results in large A_G/A_L ratio and hence large L/G. Among the modules tested, LANL 17 has the lowest packing density, and thus has the highest flow parameter.

2. Effect of packing density on separation efficiency and operational stability

From our study, we have found that the module design significantly impacts the separation efficiency and operational stability of the hollow fiber modules. To measure the separation efficiency, the height of transfer unit (HTU) is commonly used for the distillation columns. The smaller the HTU the better the separation. Due to the severe flooding problems, structured packings have not been used in the n-/iso-butane distillations. Instead staged plates are commonly used. The design HTU in those columns is equivalent to distance between two plates, which ranges from 36–60 inch (>90 cm). For the HTU of the packing columns, it can be calculated using:

$$HTU = \frac{V_G}{K * a}, \quad (3)$$

where V_G is superficial vapor velocity (cm/sec), K is overall mass transfer coefficient (cm/sec), and a is specific area of the column (cm^2/cm^3). For the flow characterization, a commonly used term is the F-factor (F_G) ($\text{m/s}(\text{kg}/\text{m}^3)^{0.5}$ /sec), which can be calculated using the superficial vapor velocity at the shell side of the column, and is related to the C-factor (C_G) (cm/sec) through the square root of the difference of liquid and vapor densities:

$$F_G = V_G \sqrt{\rho_G} \quad \text{and} \quad C_G = \frac{F_G}{\sqrt{\rho_L - \rho_G}}. \quad (4)$$

In Figure 2(a), the effect of packing density on the separation efficiency (HTU) of five LANL modules is shown. Among these five modules, LANL 17 has the least packing density (5.52%), and gives the worse performance. Due to the smallest cross-sectional area for the liquid phase in LANL 17, the liquid velocity is the highest when the gas velocity is the same among five modules. In the overall mass transfer process, the major resistance comes from the liquid side. The retention time of liquid phase in the module is more critical than that for the vapor phase. For the low packing density, the high liquid velocity results in a short retention time and thus reduces the contact time with the vapor phase. A low separation efficiency is then anticipated. Furthermore, high liquid velocities result in a large pressure drop in the liquid side for the same F-factor, as shown in Figure 2(b). In a stable operation, the pressure distribution along the hollow fiber wall between two phases is well controlled. The micro-porous wall of hollow fibers is wetted by the process fluid and holds this thin layer of liquid inside wall of the hollow fibers. Therefore, both liquid and vapor liquid phases have their own flow channels. Although the liquid pressure may be slightly higher than the vapor pressure at the top portion of the module where the liquid is fed into the module after the condenser, the vapor pressure is generally greater than the liquid pressure for the majority part of module. The problem of liquid leaking from the lumen side to the shell side of the module is insignificant. However, when the liquid pressure drop increases appreciably, the portion of the module with the liquid pressure exceeding the vapor pressure will increase. As an appreciable amount of liquid is pushed into the vapor side, it will interrupt the vapor flow and decrease stability of the operation. This reason may explain that why LANL 17 has the least stable zone for the effective separation.

As the packing density increases, the HTU decreases giving increased separation efficiency and a larger stable operating window. An explanation for this observation is the following: as the packing density increases, the cross-sectional area of the liquid phase increases. Therefore, the liquid velocity decreases, which gives a longer retention time for liquid to contact the vapor phase and hence increases the mass transfer between two phases. Simultaneously, the low liquid velocity also results in a lower pressure drop, as shown in Figure 2(b), and decreasing the likelihood of liquid being pushed into the

vapor phase. All of these changes allows for better pressure balance along the module and increases operational stability. Therefore, the high separation efficiency is obtained. For both LANL 18 and LANL 13, the HTUs of less than 30 cm are obtained when the capacity is increased to $1.0 \text{ Pa}^{0.5}$. One may expect that when the packing density increases further, higher separations (HTU < 20 cm) and wider stable zone can be achieved. However, there will be an upper-limit of the packing density. Although high packing density (up to 30%) of hollow fiber modules is commonly used in gas separation and water purification, it is not clear what the practical upper-limit for the hollow fiber modules will be for this application. Over the test range considered here (packing density up to 18.4%), appreciable increases in the vapor pressure drop were not seen. When the higher packing densities begin to appreciably increase the pressure drop on the vapor side, the upper-limit of the packing density may have been approached.

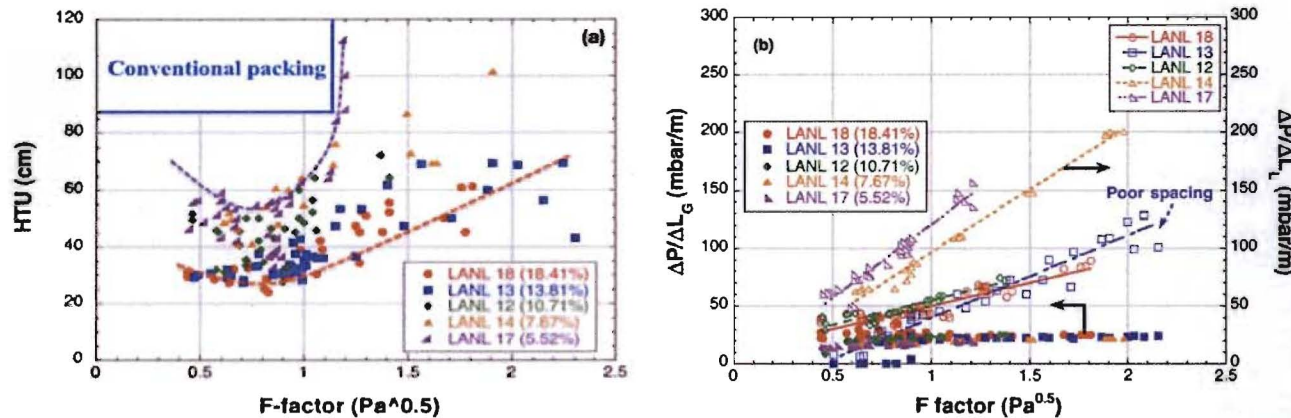


Figure 2. (a) Comparison of separation efficiency among five LANL modules and (b) The correlation between F-factor vs. pressure drop in both phases (left y-axis is the pressure drop in vapor side while right y-axis is the pressure drop in liquid side) (the operation conditions range from 15 – 40 °C, and 30 – 80 psig for n-/iso-butane system).

In Figure 2(b), we correlate the pressure drop in both phases vs. the F-factor for these five modules. As the packing density increases, the pressure drop in the liquid phase ($\Delta P/\Delta L_L$) largely decreases at the same flow capacity, and also becomes less sensitive to the increased F-factor, which will increase the operational stability. We had expected that the pressure drop in the vapor phase ($\Delta P/\Delta L_G$) would increase as the packing density increased. The experimental results suggest that the $\Delta P/\Delta L_G$ does not notably increase as the packing density increases up to 18.4%. Furthermore, the values of $\Delta P/\Delta L_G$ are less than 50 mbar/m, which are very important results. It addresses one of several engineering questions about this type of packing used in distillation applications. The pressure drop is not an engineering barrier for this type of packing materials used in olefin/paraffin distillation⁹. Interestingly, under changeable reflux conditions, the distillation experiments are not only more stable, but also give better separation compared to those obtained under the total reflux condition. An explanation to this may be the less amount of liquid traveling through the lumen side of the module reduces the likelihood of liquid leakage into the shell side, which increases the operational stability, and hence increases the separation efficiency.

3. Thermal stability study

One of the concerns about the polymeric materials using as the structured packing is their durability when they are continually exposed in the organic solvent environment. The hollow fibers must maintain their mechanical integrity and morphology for the lifetime of the hollow fiber modules. Therefore, we have conducted two-year long thermal stability of polypropylene (PP) hollow fibers. We have aged the fibers in several organic solvents at elevated temperatures for up to two years. In Figure

3, we summarize the TGA results for the polypropylene (PP) soaked in benzene and cyclohexane at 50 °C up to 24 months (a) and in iso-/n-butane under distillation condition (b). The TGA results suggest that PP thermally decompose above 350 °C. Although the organic solvent exposure does not change their thermal stability appreciably, PP fibers are not recommended to use at temperature above 100 °C.

The TGA results show a slight weight gain before the PP decomposition instead of a weight loss, which is not commonly observed. This weight gain may be due to experimental error. The fine PP fibers experience static repulsion, which makes loading sufficient quantities of sample (>1mg) into a TGA pan difficult. The slight weight gains during heating are most likely due to convection within the TGA furnace. When small samples are used, the convection current from heating gives the false impression of weight gain. Nevertheless, the TGA behaviour of PP fibers does not significantly change upon the solvent exposure process.

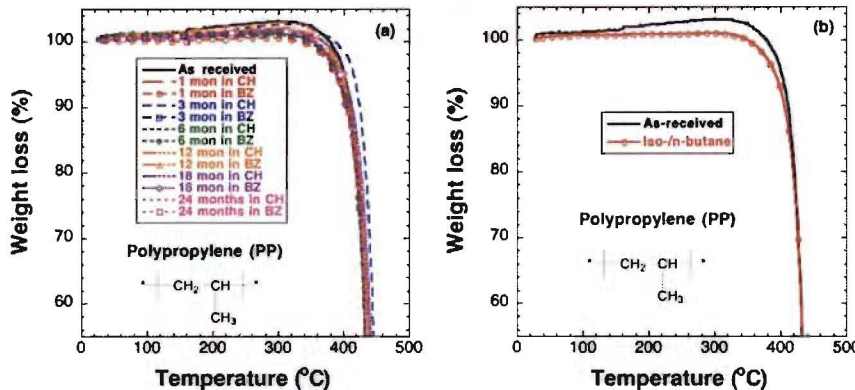


Figure 3. The TGA results for PP fibers immersed in benzene (BZ) and cyclohexane (CH) at 50 °C for different times (a) and for PP fibers exposed in C₄ distillation condition (b).

The DSC results for the PP fibers exposed to various solvents are summarized in Table 1. The reported T_g for PP is -3 °C¹⁰, however for all of the samples, there was no discernable glass transition observed between -30 and 40 °C. The lack of the observed T_g could be due to the high crystallinity, which tends to decrease the magnitude of the heat flow change at T_g, as well as to broaden the T_g so that the transition is indistinguishable from the baseline. For all samples, the only observed transition was a melting endotherm between 120 and 180 °C. While the peak in the melting endotherm did not change significantly with either solvent or aging, there were changes in the level of crystallinity. For both solvents the level of crystallinity initially increases and then after 12 months remains relatively constant.

Table 1. Summary of DSC results for as-received and treated PP membranes.

| Sample History | T _m (°C) | ΔH _f (J/g) | % Cryst |
|---|---------------------|-----------------------|---------|
| As received | 160 | 90.3 | 43 |
| After cool | 159 | 105 | 51 |
| 12 month in C ₄ at room temp. | 161 | 103 | 50 |
| Exposure to cyclohexane at different times at 50 °C | | | |
| 1 month | 161 | 69.5 | 34 |
| 3 month | 161 | 87.9 | 43 |
| 6 month | 161 | 96.6 | 47 |
| 12 month | 161 | 106 | 51 |
| 18 month | 161 | 101 | 49 |
| 24 month | 161 | 105 | 51 |
| Exposure to benzene at different times at 50 °C | | | |
| 3mo Benzene 50C | 161 | 95.8 | 46 |

| | | | |
|----------|-----|-----|----|
| 6 month | 161 | 73 | 45 |
| 12 month | 162 | 105 | 51 |
| 18 month | 161 | 102 | 49 |
| 24 month | 161 | 103 | 50 |

Dynamic mechanical analysis (DMA) was employed to examine the effect of solvent exposure on the mechanical properties of the PP hollow fibers. If solvent exposure causes a change in the polymer's crystalline structure, the mechanical properties of the membrane should reflect these changes. For each sample, an oscillatory strain was applied to the membrane in tensile mode and the resultant stress was measured. The oscillatory nature of the test allows us to probe both the elastic and viscous components of the material and obtain the complex modulus, $E^* = E' + iE''$, where E' is the storage modulus (elastic component) and E'' is the loss modulus (viscous component).

In Figure 4(a), the DMA results of PP fibers are presented after they were exposed to liquid C_4 under the distillation conditions. Oscillatory strain sweeps beginning at 0.01% strain and continuing until breakage were applied to each sample at a frequency of 1 Hz. In Figure 4(a), the slope of the line at low strains represents the Young's modulus. In this case, the modulus is relatively unaffected by the exposure time. The point at which the slope change marks the transition from a linear viscoelastic response (to the applied strain) to a non-linear response. The results suggest that the strain at which this transition occurs slightly increases after 12 months exposure. The storage (elastic) and loss (viscous) components of the modulus are shown in Figure 4(b). The results suggest that the soaked PP not only gives a slightly higher strain, but also gives higher storage and loss modulus.

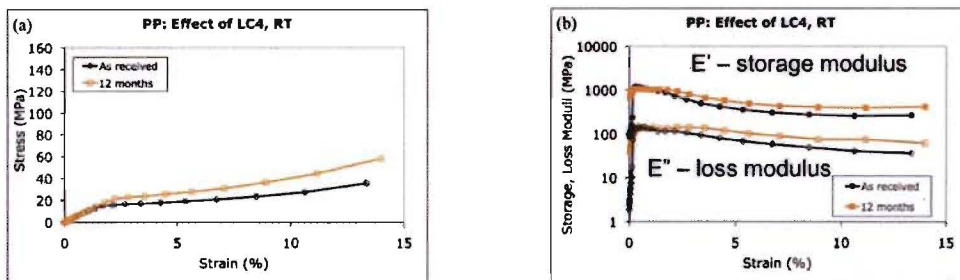


Figure 4. The oscillatory strain sweep (a) and storage vs. strain (b) of PP fibers before and after they were exposed to liquid C_4 for 12 months.

The results of the cyclohexane exposure are shown in Figure 5 where the slope of these lines is relatively unaffected by the exposure time. The transition point stays more or less the same. However, the strain at the breaking point does change with the exposure time. In the first 12 months, the breaking strain gradually increases as the exposure time increases. After the strain reaches its largest values for this increase, $\sim 17\%$, it starts to decrease slightly after 24 month exposure. Overall, the behavior of stress vs. strain of PP fibers does change.

From both SEM and BET results (not shown), one notices some rearrangement of the material's pore structure: the pores become smaller from 0 – 3 months and then begin to shift back to larger sizes in the meso-pore range. Correspondingly, the correlation of storage (loss) modulus vs. strain, as shown in Figure 5(b), also changes. However, comparing the 24-month exposure data, we find that the DMA data is almost identical to that of the 12-month exposure sample. However, the rearrangement of the pore morphology and crystallinity may be responsible for the changes seen in the stress-strain data.

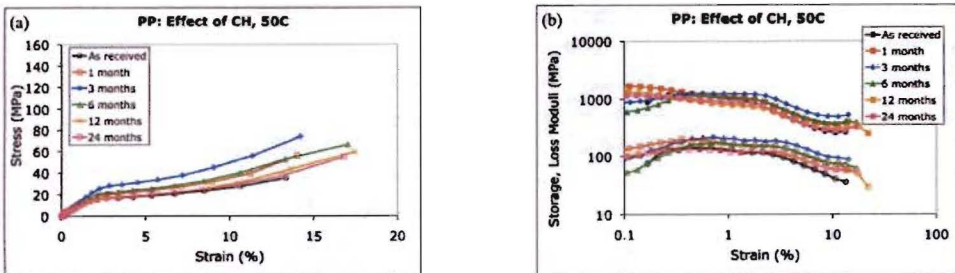


Figure 5. The oscillatory strain sweep (a) and storage vs. strain (b) of PP fibers before and after they were exposed to cyclohexane at 50 °C for different times.

Upon the benzene exposure, an appreciable changes in both stress vs. strain behavior and modulus are observed, as shown in Figure 6(a) and 6(b), respectively. As the membrane becomes denser over the exposure process, that is seen in the SEM characterization (not shown here), the Young's modulus of the treated samples increases appreciably. The 24 month sample gives the largest Young's modulus together with the highest storage and loss modulus.

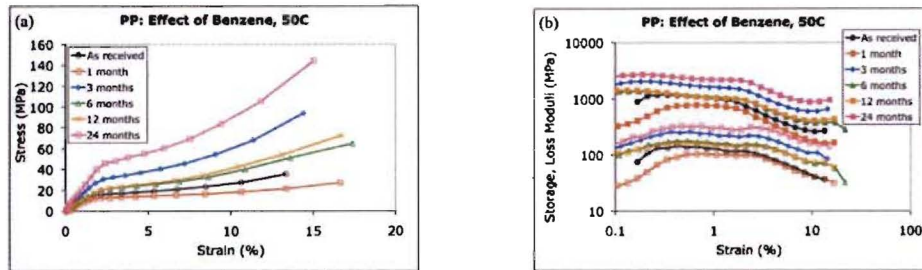


Figure 6. The oscillatory strain sweep (a) and storage vs. strain (b) of PP fibers before and after they were exposed to benzene for different time at 50 °C.

From the above study, we conclude that PP fibers are stable at iso-/n-butane environment for a long period of time. Therefore, polypropylene fibers are suitable for the structured packings in ethane/ethylene, propane/propylene, and iso-butane/n-butane distillations, but not for the aromatic environments.

Conclusion

In this scaled-up system, we demonstrate that the high separation efficiency (HTU < 30 cm) and a long-term stable operation (> 9 months) are achieved using hollow fiber as structured packings for the iso-/n-butane distillation. When the F-factor is up to $2.2 \text{ Pa}^{0.5}$, the pressure drop in the vapor side is below 50 mbar/m. This important result confirms that the pressure drop is not an engineering barrier for hollow fiber to be used as structured packings in the distillation columns. We conclude that the packing density is an important parameter for the module design to warrant the stability and the separation efficiency. The preliminary results on two lab-scaled systems show the great improvement on the separation efficiency and the apparatus capacity using hollow fibers as structured packings over the conventional packings in the olefin/paraffin distillation.

However, as the system is further scaled up, the length of the column increases. The pressure distribution along the column length will be critical to the operational stability. In addition to the packing density, the morphology of hollow fibers will play an important role in the module design to maintain the uniform pressure distribution between two phases, and thus ensure the separation efficiency and the operational stability. We may encounter more engineering challenges as the apparatus is further scaled into a pilot plant scale, the perspective of this technology is still attractive.

Acknowledgement

We gratefully acknowledge DOE office of Energy Efficiency and Renewable Energy – ITP program for funding this work. We would like to thank Professors Cussler and Sirkar for their intriguing discussions and scientific insights about this technology. We would like to thank some support from Chevron Company. Finally, we would like thank Dr. Malcolm Morrison for providing fruitful discussions on the hollow fiber module design and a marketing perspective on the hollow fiber industry.

References

1. Eldridge, R. B., Olefin/paraffin Separation Technology: A Review. *Ind. Eng. Chem Res.* **1993**, 32, 2208-2212.
2. Chapas, R.; Colwell, J. A. *Industrial Technologies Program Reserach Plan for Enerngy-Intensive Process Industries*; Battelle: 2007.
3. Angelini, P.; Armstrong, T.; Counce, R.; Griffith, W.; LKlasson, T.; Muralidharan, G.; Narula, C.; Sikka, V.; Closset, G.; Keller, G.; Watson, J. *Materials for Speartion Technologies: Energy and Emission Reduction Opportunites*; DOE, EERE Office: Washington, D. C., May 4, 2005; p 103.
4. Kister, H. Z., *Distillation - Design*. McGraw Hill: New York, 1992.
5. Yang, D.; Barbero, R. S.; Devlin, D. J.; Cussler, E. L.; Colling, C. W.; Carrera, M. E., Hollow fibers as structured packing for olefin/paraffin separations. *J. Membr. Sci.* **2006**, 279, (1-2), 61-69.
6. Sirkar, K. K., Membranes, phase interfaces, and separations: Novel techniques and membranes-an overview. *Industrial and Engineering Chemistry Research* **2008**, 47, (15), 5250-5266.
7. Yang, D.; Devlin, D. J.; Barbero, R. S., Effect of hollow fiber morphology and compatibility on propane/propylene separation. *J. Membr. Sci.* **2007**, 304, (1-2), 88-101.
8. Yang, D.; Matinez, R.; Fayyaz-Najafi, B.; Wright, R., Light hydrocarbone distillation using hollow fibers as structured packings *J. of Membrane Science* **2010**, 362, 11.
9. Olujic, Z.; Behrens, M.; Sum, L.; Fakhri; Graauw, J. d., Augmenting distillation by using membrane based vapor-liquid contactors: An engineering view from Delft. *J. of Membrane Science* **2010**, 13.
10. Wunderlich, B., *Thermal Analysis of Polymer Materials*. Springer-Verlal: Berlin, Heidelberg, 2005.